*Ceramics International* **24** (1998) 53–59

PII: S0272-8842(96)00077-6
0272-8842/97 $17.00+.00

# High-Temperature Vaporization of $Li_2O$ Component from Solid Solution $Li_xNi_{1-x}O$ in Air

**Toshiyuki Sata***

Department of Industrial Chemistry, Kumamoto Institute of Technology, Ikeda, Kumamoto 860, Japan

(Received 23 February 1996; accepted 28 August 1996)

**Abstract:** The vaporization experiments for $Li_2O$ component from disk type specimens of the solid solution $Li_xNi_{1-x}O$ ($x \leq 0.4$) (materials for the fuel cell) were carried out in flowing air (1 $cms^{-1}$) in the temperature range 400–700°C. Log–log plots of the vaporization vs time consisted of two or three straight lines with different slopes (0.2–0.97). The smaller slopes at 500–600°C, as shown later, suggest a growth of concentration gradient of $Li_2O$. The slope at the second stage increased to unity with an increase in $x$ from the starting value and with lowering temperature for the same $x$. The vaporization stopped at the third stage, leaving some $Li_2O$ behind. From considerations of the change in $x$-value with time, a formation of a $Li_2O$ concentration gradient in the specimen, and an activation energy for the vaporization, a formation reaction of $Li_2O_2$(g) from $Li_2O$(c) decomposed from the solid solution and its diffusion rate in the specimen are supposed to be rate-determining. © 1997 Elsevier Science Limited and Techna S.r.l.

## 1 INTRODUCTION

In the system Ni–O, three oxides (NiO, $Ni_2O_3$ and $NiO_2$) are known.[1,2] In the system between $Li_2O$ and respective Ni-oxides, the two-component double oxides $Li_2NiO_2$,[3] $LiNiO_2$[4] and $Li_2NiO_3$[5] have been shown to exist, as represented in Fig. 1. Reactions between $Li_2O$ and NiO, in air or oxygen atmosphere, lead to the formation of the $Li_xNi^{2+}{}_{1-2x}Ni^{3+}{}_xO$ solid solution, in which the oxidation state of Ni changes from +2 to +3.[4,6,7] The values of $x$ in the solid solution lie between 0 and 0.5 (from NiO to $LiNiO_2$). The formation of this solid solution and the substitution of Li at Ni sites has been studied since 1950, with the aim to increase the electrical conductivity of NiO[8,9] and to manufacture electrode materials for fuel cells or secondary cells.[9–13] The lattice constant of NiO with the NaCl-type structure decreases with additions of Li within the above solid solution series $Li_xNi_{1-x}O$. The NaCl structure is maintained up to an $x$-value of 0.3, and then it changes to a rhombohedral (hexagonal) form at 0.4 or 0.5.[4,6,7] Thus, the values of $x$ can be determined from the cell volumes of the NaCl lattice ($x < 0.3$) and rhombohedral lattice ($x > 0.3$) using a linear relationship between cell volume and composition $x$ (from $7.29 \times 10^{-2}$ $nm^3$ for $x=0$ to $6.79 \times 10^{-2}$ $nm^3$ for $x=0.5$),[6,14] as shown in Fig. 2.

Several investigations[15–17] on sintering for the solid solution with $x$-values of 0.06–0.44 have been performed to fabricate porous electrodes. The sintering temperatures were between 700 and 900°C. In these sintering studies, mixtures of metallic Ni and $Li_2CO_3$ have been used as the starting materials, and the presence of a small amount of $Li_2CO_3$ melt was found to be effective in acquiring higher densities. Loss of $Li_2O$ due to vaporization became serious above 900°C. Studies on the vaporization of the Li component during the sintering process have been performed[14,18–25] for solid solutions with $x$-values of 0.12–0.5, in the temperature range 650–880°C. Since these studies were not systematic, the vaporization of the sintered bodies within the solid solutions were investigated in this study.

Present contact address (after retirement): D7-504, 1-28-16 Unomori, Sagamihara, Kanagawa 228, Japan.

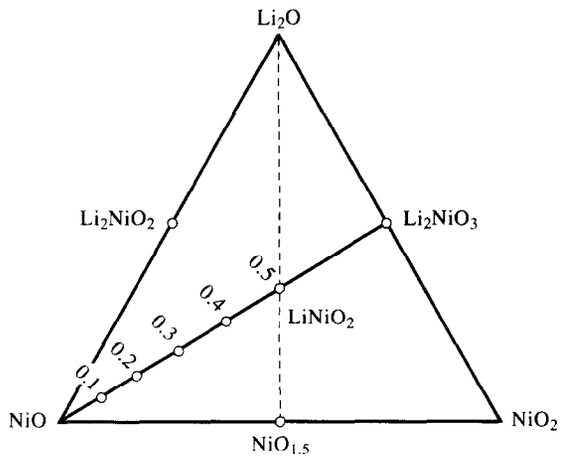


**Fig. 1.** The system $Li_2O$–NiO–$NiO_2$. The $x$-values of 0.1–0.5 are those in the solid solution $Li_xNi_{1-x}O$.

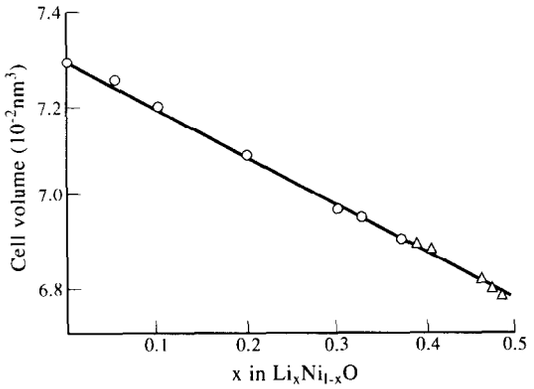


**Fig. 2.** Linear relation of cell volume of NaCl type (○) and rhombohedral (△) lattice with $x$-value in the solid solution $Li_xNi_{1-x}O$ by Goodenough *et al.*[6]

## 2 EXPERIMENTAL

### 2.1 Synthesis and sintering

Special-grade reagents of $Li_2CO_3$ and NiO were dried and mixed in an agate mortar with acetone so as to have atomic ratios of Li:Ni of 1:9, 2:8, 3:7 and 4:6. The mixed powders were pressed to a rectangular bar (3.1 cm × 1 cm × 0.5 cm) at 100 MPa. These bars were fired in flowing oxygen (200 $cm^3min^{-1}$) at 500–800°C for 6–72 h in an alumina boat. The reaction products generally contained small amounts of unreacted $Li_2CO_3$ and NiO. In order to determine the $x$-value of the produced solid solution powders, the linear relationship between the cell volume and $x$ mentioned above (Fig. 2) was used.[6,14,26] Three peaks at (220), (311) and (222) in the XRD pattern were used for both the unreacted NiO and the cubic solid solution, and both combinations (113)–(0012) and (116)–(018) were used for the rhombobedral solid solution.

After the synthesis process, the powders were pressed to disks (1.34 cm in diameter and 0.2 cm thick) at 100 MPa. These disks were sealed in a flat stainless steel tube, closed by pressing at both ends to prevent loss of Li, and then sintered at 700–900°C for 2–3 h.

### 2.2 Vaporization

The surface of the sintered disk was polished by sand paper and an agate plate and then washed ultrasonically in acetone. An area of the outer surface (3.1–3.7 $cm^2$) of the disk specimen was obtained, with both diameter and thickness measured with a micrometer ($10^{-4}$ cm). A specimen was placed on a mullite boat and inserted in the mullite reaction tube (2 cm inner diameter) of a SiC furnace, kept at a constant temperature and then heated in flowing air (200 $cm^3min^{-1}$ or 1 $cms^{-1}$ at NTP) passed through both silica gel and NaOH granules. This flow rate (200 $cm^3min^{-1}$) was used so that the weight loss ($10^{-4}$–$10^{-3}$ g) could be measured precisely. The weight loss due to the vaporization is proportional to the flow rate.[27] After being kept at 400°C to stabilize the weight (i.e. until the weight was constant), the specimen temperature was raised to the test temperature. The specimen was rapidly cooled after the experiment and the weight loss was measured with a microbalance (Sartorius AG, $10^{-6}$g in sensitivity). The vaporization per unit surface area ($gcm^{-2}$) was calculated. The $x$-values after vaporization were obtained by the above-mentioned XRD method from the surface to the interior of the disk specimen. XRD patterns of the interior were examined for each face after successive shavings. The depth from the surface was measured with a micrometer ($10^{-4}$ cm).

## 3 RESULTS AND DISCUSSION

### 3.1 Synthesis and sintering

In repeated firings — every 24 h at 500°C for mixed powders with $x = 0.1$ and 0.2, and at 600°C for those with $x = 0.3$ and 0.4 — in flowing oxygen (50 $cm^3min^{-1}$), the $x$-value of the specimen surface increased from the original value of the starting mixture at an early stage and then decreased with time to the original $x$-values, except for $x = 0.4$, as shown in Fig. 3. The amount of unreacted NiO decreased with time, but it did not, however, disappear completely, even after 120 h. The lattice constant of NiO increased from 0.4170 nm within

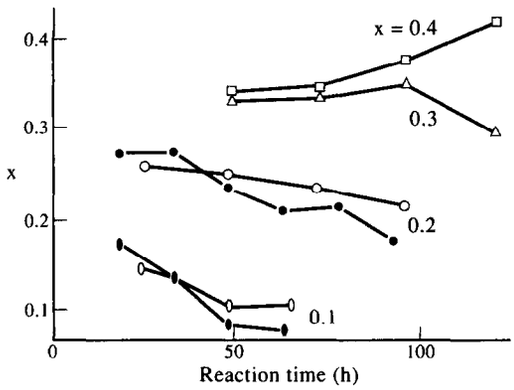


**Fig. 3.** Change in $x$-value of the reaction products at 500°C ($x=0.1$ and 0.2) and 600°C ($x=0.3$ and 0.4) with time. Black plots show repeated firing for 15 h and white plots show repeated firings for 24 h. The $x$-values on the respective curves represent those of the starting specimens.

the first 20 h, followed by a constant (maximum) value of 0.4185 nm. The above-mentioned results for the synthesis from $Li_2CO_3$ and NiO agree well with those in the literature.[6,14,18,28] From the above results, the reaction at 800°C for 2 or 3 h in an oxygen atmosphere was found to be the best.

The formation reaction of the solid solution from both oxides is written in the following equation:[6]

$$\frac{x}{2}Li_2O + (1-x)NiO + \frac{x}{4}O_2 = Li_xNi_{1-2x}Ni_x^{3+}O \quad (1)$$

To make the solid solution, $Ni^{2+}$ is oxidized to $Ni^{3+}$ by 1/2 $O_2$ per mole of $Li_2O$, with the substitution of $Li^+$ at the Ni sites. Accordingly, the oxygen atmosphere promotes the solid solution formation. The rapid increase of $x$ on the surface in the early stage, followed by the gradual decrease as shown in Fig. 3, is explained as follows. The $Li_2O$ component first reacts at the surface rich in oxygen gas to form a solid solution rich in $x$, leaving unreacted NiO in the bulk. Then the dissolution proceeds to the interior of the NiO grains, decreasing to an average value of $x$. At higher temperatures, it is thought that the vaporization of $Li_2O$ from the surface takes place at the same time.

Sintering experiments were performed at temperatures from 700 to 900°C for 2–3 h in the sealed stainless steel tube. Relative densities of the sintered bodies were about 74% for $x=0.1$ and almost 100% for $x=0.2$, 0.3 and 0.4 at 800–850°C for 2 h. Theoretical densities of the solid solutions are given in the literature.[4,11]

### *3.2 Vaporization*

The sintered disks with $x$-values of 0.1, 0.2, 0.3 and 0.4 were heat-treated in a constant air flow of 200 $cm^3min^{-1}$. Results of log vaporization (weight loss in $gcm^{-2}$) vs log time (s) are shown in Fig. 4. The presence of two or three stages is found in all the experiments. The first stage with a lower slope is seen at the lower temperatures of 500 and 600°C. The second stage has higher slopes, which are dependent on the $Li_2O$ contents and temperatures. In the third stage, the vaporization stopped. This situation differs from the usual vaporizations, in which the diffusion of an ion of a vapour species is rate-determined and the slope value decreases in the next stage. The slope of less than unity in the first and second stages is evidence of the presence of a resistance inhibiting the vaporization from the surface. The slopes in the first and second stages vs $x$-values of the original specimens at 400–700°C are plotted in Fig. 5. These slopes increase with increasing $x$-values. This means that the vaporization process approaches a constant rate with increasing $x$-value.

Figure 6 shows changes in $x$-value on the surface with time at 500 and 600°C. The $x$-value on the surface of the starting specimen with $x=0.1$

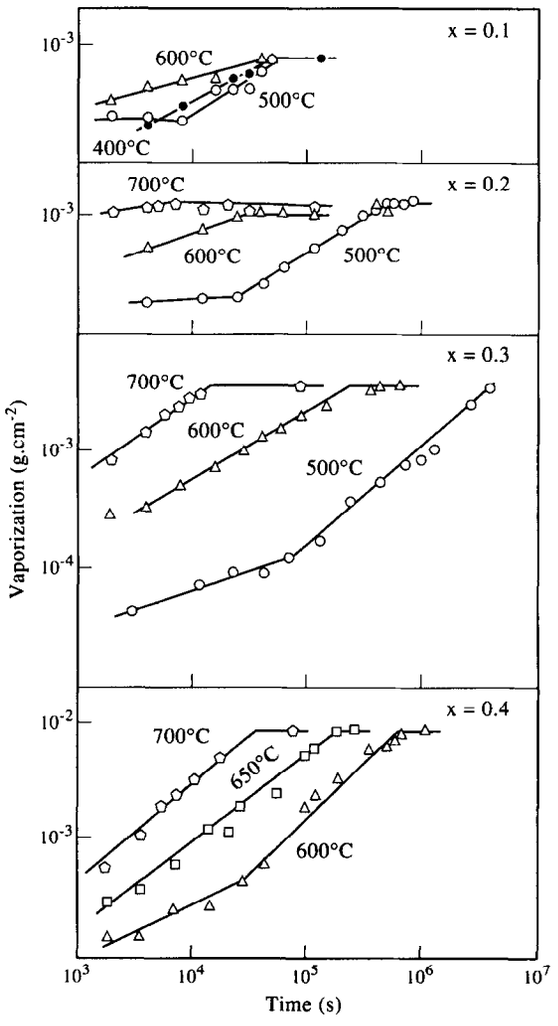


**Fig. 4.** Vaporization weight loss with time for specimens with $x=0.1$, 0.2, 0.3 and 0.4.

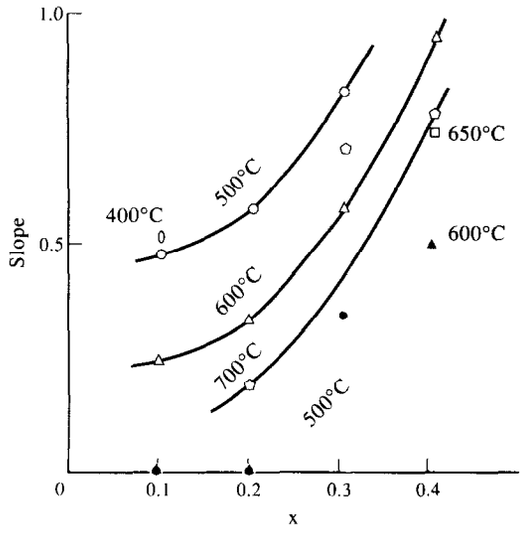


**Fig. 5.** Change in slope of the second stage in the vaporization in Fig. 4. Black plots are those for the lower slopes in the first stage.

increased to 0.25 within 3 h at 500°C, that for the specimen with $x=0.2$ increased to 0.3 in 50 h at 500°C, that for the specimen with $x=0.3$ increased to 0.44 in 5 h at 600°C, and that for the specimen with $x=0.4$ increased to 0.49 at 600°C. It shows that there is $Li_2O$ enrichment in the solid solution at the surface in the early stage, which then decreases due to the vaporization. The lower slope values, as seen at 500 and 600°C, related to the increase in $Li_2O$ content at the vaporization surface. As shown in Fig. 7, the $x$-values of the solid solution after the vaporization experiments decreased linearly with depth into the interior of the specimen, indicating an inverse gradient against that observed in usual ion-diffusion-controlled processes. This means that the $x$-value in the solid solution has a higher value than in the bulk because of the higher oxygen content over the surface and the diffusion rate of $Li^+$ to the vaporization surface may he fairly high. But the diffusion rate in the solid solution body has not yet been reported.

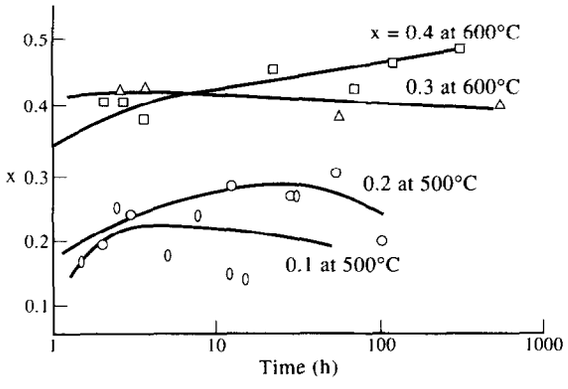


**Fig. 6.** Change in $x$-value of the vaporized surface with time.

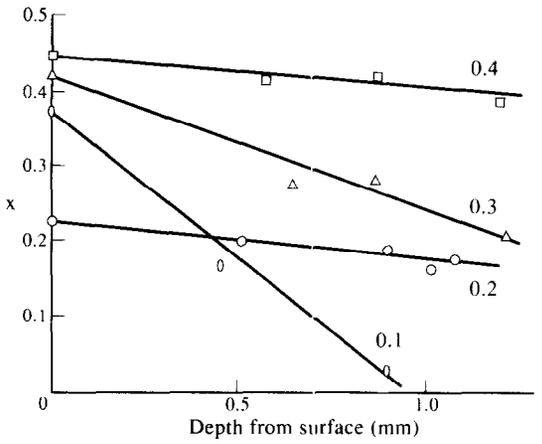


**Fig. 7.** Distribution of $x$-values from the surface to the centre of the specimen (same as shown in Fig. 6) after the vaporization at 500°C (for $x=0.1$ and 0.2) and 600°C (for $x=0.3$ and 0.4).

Arrhenius plots of the vaporization rates at the starting time of the second stage vs $1/T$ are represented in Fig. 8. Similar values of the activation energy ($344 \pm 5\,kJmol^{-1}$) are obtained for all specimens, even with different $x$-values. The vaporization reaction of the $Li_2O$ component from the solid solution can be written as follows:

$$Li_xNi^{2+}_{1-2x}Ni^{3+}_xO = a[Li_yNi^{2+}_{1-2y}Ni^{3+}_yO] + bLi_2O(g) + cO_2 \quad (2)$$

where $a=(1-x)/(1-y)$, $b=(x-y)/2(1-y)$ and $c=(x-y)/4(1-y)$ for $x>y$. The vaporization weight loss corresponds to the sum of $bLi_2O$ and $cO_2$. Since $b/c$ is equal to 2, this vaporization loss is proportional to that of $Li_2O$ and corresponds to that of $bLi_2O_2(g)$ as follows. Solid $Li_2O(s)$ was not

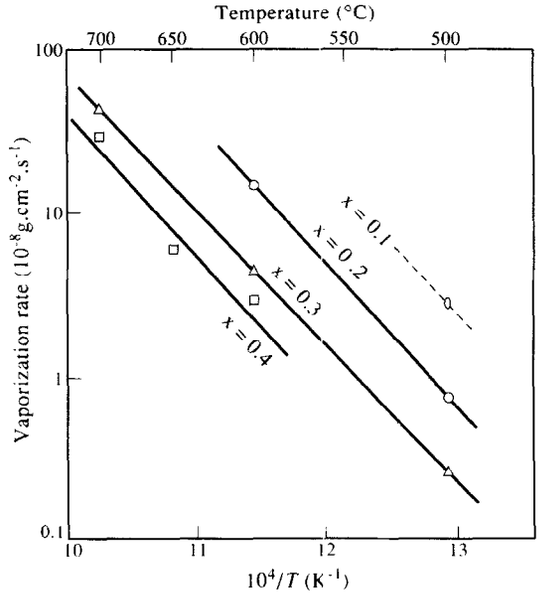


**Fig. 8.** Arrhenius plots of vaporization rates at the starting time of the second stage against $1/T$.

detected in the X-ray pattern. Vapour pressures of the gaseous oxide species from solid alkaline oxides in oxidizing atmospheres were described.[29] At 1 000 K and a $p_{O_2}$ of 0.2 bar, the vapour pressure of $Li_2O_2$(g) is $2.7\times10^{-6}$ Pa, LiO(g) is $6.2\times10^{-8}$ Pa and $Li_2O$(g) is $3.1\times10^{-8}$ Pa over $Li_2O$(c). This indicates the maximum pressure of the peroxide vapour (96%). The following heats of reaction are cited.[30]

$$Li_2O(c) = 2Li(c) + \frac{1}{2}O_2 \quad + 598.73\ kJmol^{-1} \qquad (3)$$

$$2Li(c) + O_2 = Li_2O_2(g) \quad - 242.67\ kJmol^{-1} \qquad (4)$$

Thus, the heat of sublimation of $Li_2O$(c) to $Li_2O_2$(g) in air is calculated to be 356 $kJmol^{-1}$. The obtained activation energy (344 $kJmol^{-1}$) is similar to this value.

As indicated in Fig. 7, $Li_2O$ concentrations on the vaporization surface are higher than those in the bulk. Grain boundary segregation from the solid solution of $Li_xNi_{1-x}O$ containing up to 3 at% Li ($x=0.03$) at 900°C was reported.[31] Segregation (very thin) of $Li_2O$ at the grain boundaries increases at higher temperature and lower $p_{O_2}$. Since a heat of solution of 40 $kJmol^{-1}$ for Li to the solid solution was reported,[31] a rate-determining step for the vaporization rate is supposed to be the formation reaction of $Li_2O_2$(g) from $Li_2O$(c).

In the first kinetic study on the vaporization from the solid solution,[21] the vaporization from a specimen with an $x$-value of 0.13 was conducted above 1000°C and the square of the vaporization rate was proportional to time (corresponding to 0.5 of the slope). The activation energy was 209 $kJmol^{-1}$ in the temperature range 1200–1400°C. This value differs from that of the present report in the temperature range where the decomposition of the solid solution is considerable. The second report[20] described specimens with $x$-values of 0.193 and 0.3 prepared from Ni and $Li_2CO_3$ that were heat-treated at 800°C for 350 h and these $x$-values decreased with time. This report indicated rapid increases in $x$-values at the initial time. This is the same result as that indicated in Fig. 6. Another thermogravimetric measurement,[19] for specimens with $x$-values of 0.25, 0.4 and 0.5, reported a weight increase at 400–650°C and a weight decrease at 735–883°C.

The transfer times from the first to the second stage (dotted line) and from the seconnd to third stage (solid lines) are plotted against the vaporization temperatures in Fig. 9. These transfer times increase with increasing $x$-value and with lower vaporization temperature. The transfer time from

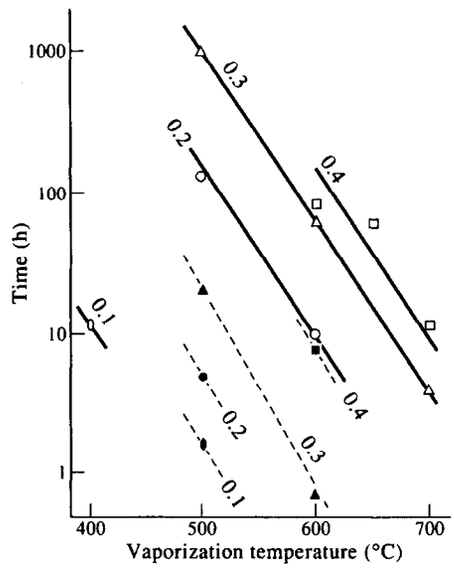


**Fig. 9.** Time of transfer from first to second (dotted lines) and from second to third stage (solid lines) of vaporization for respective $x$-values of starting materials vs vaporization temperatures.

the first to the second stage corresponds to the maximum of the curves for the respective $x$-value in Fig. 6. Accordingly, the first stage is the process of increasing $x$-value in the solid solution at the surface, accompanied by the formation of the $Li_2O$ concentration gradient. Therefore, in this first stage, only a small vaporization was observed. In the second stage, it is supposed that the formation and diffusion of $Li_2O_2$(g) are related to the rate-determining step.

The vaporization stopped in the third stage, because such an inverse concentration gradient of $Li_2O$ was completed. The vaporization (in %) of $Li_2O$ against the original total amount of $Li_2O$ and the $x$-value at the beginning of the third stage, where the vaporization stopped, are calculated. These results show the same weight loss in % and $x$-value at all temperatures for a starting specimen with the same $x$-value: 24%–0.024 of $x$ for the specimen with 0.1 of $x$, 17%–0.034 for 0.2 of $x$, 31%–0.093 for 0.3 of $x$ and 50%–0.20 for 0.4 of $x$, as average values. They show that the vaporization stopped before the complete vaporization of the original amount of $Li_2O$. This feature can be understood by completion of the inverse gradient of $x$. It is thought that the dissolution equilibrium in the solid solution at $p_{O_2}$ of air may be attained when the vaporization stops. Such a dissolution equilibrium for reaction (2) was described,[31] but it should be investigated in more detail at temperatures between 500 and 700°C under various $p_{O_2}$. In the study by Iida,[21] above 1000°C the temperature effect for the reaction was higher than the $p_{O_2}$ effect and the vaporization was continued.

## 4 CONCLUSION

Solid solutions of $Li_xNi^{2+}{}_{1-2x}Ni^{3+}{}_xO$, with $x$-values of 0.1, 0.2, 0.3 and 0.4, were synthesized from $Li_2CO_3$ and NiO at 500–800°C in an oxygen flow. Green compacts of these synthesized powders were sintered at 800–850°C in a sealed stainless steel tube. These sintered disk specimens were subjected to vaporizations in flowing purified air ($200\,cm^3min^{-1}$) at temperatures between 400 and 700°C. Log–log plots of vaporization weight loss per unit surface area vs time at each temperature consist of two to three straight lines. The slopes (0.20–0.97) in the first and second stages tend to unity with increasing $x$ and decreasing temperature. In the third stage, the vaporization stopped. The $x$-values of the surface measured after vaporization rapidly increased at the initial stage of the vaporization, followed by a decrease with time. The $x$-values in the specimens decreased linearly from the surface to the interior along the specimen thickness. An activation energy of $344\,kJmol^{-1}$, obtained for the initial time of the second stage, corresponds to the heat of reaction from $Li_2O(c)$ to $Li_2O_2(g)$ vapour. From the increase in slope value for the respective stage, the inverse gradient of $x$ (higher concentration of Li at the surface) and halt of the vaporization at the third stage, the formation of $Li_2O_2(g)$ from $Li_2O(c)$ and its diffusion in the body may be related to the rate-determining step in the vaporization, not the diffusion of Li ions, but this has yet to be confirmed. More data on the solid solution are needed: the formation and decomposition rate, thermochemical data, solubility relation at various temperatures and $p_{O_2}$, diffusion rate of Li ions, etc.

## ACKNOWLEDGEMENTS

The author would like to thank Mr M. Kagami and Mr T. Miyaoka for their collaboration in these experiments.

## REFERENCES

1. BOGATSKI, D. P., The system Ni–$O_2$. *Zhur. Obshchei Khim.*, **21** (1951) 9.
2. BOGATSKI, D. P., *Phase Diagrams for Ceramists*. The American Ceramic Society, Columbus, OH, 1964, Fig. 16.
3. RIECK, H. & HOPPE, R., Ein neues oxoniccolat: $Li_2NiO_2$. *Z. Anorg. Allg. Chem.*, **392** (1972) 193–196.
4. PERAKIS, N. & KERN, F., Sur la structure et le comportement magnetique de l'oxyde de nickel additione d'ions lithium. *Compt. Rend.*, **269B** (1969) 281–284.
5. DYER, L. D., BORIE, B. S., Jr & SMITH, G. P., Alkali metal–nickel oxides of the type $MNiO_2$. *J. Am. Chem. Soc.*, **76** (1954) 1499–1503.
6. GOODENOUGH, J. B., WICKHAM, D. G. & CROFT, W. J., Some magnetic and crystallographic properties of the system $Li_xNi_{1-2x}Ni_xO$. *J. Phys. Chem. Solids*, **5** (1958) 107–116.
7. MIGEON, H. N., ZANNE, M., GLEITZER, C. & AUBRY, J., The $Li_2O$–NiO–$O_2$ system at 670°C and the consequences of non-stoichiometry on the magnetic properties of the $Li_xNi_{1-2x}O_{1+y}$. *J. Mater. Sci.*, **13** (1978) 461–466.
8. VERWEY, E. J., HAAYMAN, P. W., ROMEYN, F. C. & VAN OOSTERHOUT, G. W., Controlled-valency semiconductors. *Phillips Res. Rep.*, **5** (1950) 173–187.
9. TICHENOR, R. L., Nickel oxides: relation between electrochemical reactivity and foreign ion content. *Ind. Eng. Chem.*, **44**(5) (1952) 973–977.
10. BAUMGARTNER, C. E. & ZARNOCH, K. P., Fabrication and characterization of porous lithium-doped nickel oxide cathodes for use in molten carbonate fuel cells. *Am. Ceram. Soc. Bull.*, **64**(4) (1985) 593–597.
11. ANTOLINI, E., LEONINI, M., MASSAROTTI, V., MARINI, A., BERBENNI, V. & CAPSONI, D., On the role of lithium carbonate in the preparation of doped nickel oxide cathodes for molten carbonate fuel cells. *Solid State Ionics*, **39** (1990) 251–261.
12. EBNER, W., FOUCHARD, D. & XIE, L., The $LiNiO_2$/carbon lithium-ion battery. *Solid State Ionics*, **69** (1994) 238–256.
13. BRANDT, K., Historical development of secondary lithium batteries. *Solid State Ionics*, **69** (1994) 173–183.
14. PICKERING, I. J., LEWANDOWSKI, J. T., JACOBSON, A. J. & GOLDSTONE, J. A., A neutron powder diffraction study of the ordering in $Li_xNi_{1-x}O$. *Solid State Ionics*, **53-56** (1992) 405–412.
15. ANTOLINI, E. & GIORDANI, M., Effect of lithium carbonate on the densification of $Li_xNi_{1-x}O$ solid solutions at temperatures up to 900°C. *Mater. Lett.*, **12** (1991) 117–122.
16. ANTOLINI, E., Sintering of $Li_xNi_{1-x}O$ solid solution at 1200°C. *J. Mater. Sci.*, **27** (1992) 3335–3340.
17. ANTOLINI, E., Effect of the method of obtaining $Li_2CO_3$–$Li_yNi_{1-y}O$ mixtures on the densification of the resulting $Li_xNi_{1-x}O$ solid solutions. *Ceram. Int.*, **18** (1992) 399–402.
18. IIDA, Y., Time dependence of NiO–$Li_2O$ solid solution formation. *J. Am. Ceram. Soc.*, **43** (1960) 117–118.
19. MARINI, A., MASSAROTTI, V., BERBENNI, V., CAPSONI, D., RICCARDI, R., ANTOLINI, E. & PASSALACQUA, B., On the thermal stability and defect structure of the solid solution $Li_xNi_{1-x}O$. *Solid State Ionics*, **45** (1991) 143–155.
20. BERBENNI, V., MASSAROTTI, V., CAPSONI, D., RICCARDI, R., MARINI, A. & ANTOLINI, E., Structural and microstructural study of the formation of the solid solution $Li_xNi_{1-x}O$. *Solid State Ionics*, **48** (1991) 101–111.
21. IIDA, Y., Evaporation of lithium oxide from solid solution of lithium oxide in nickel oxide. *J. Am. Ceram. Soc.*, **43** (1960) 171–172.
22. BRONGER, W., BADE, H. & KLEMM, W., Zur Kenntnis der Niccolate der Alkalimetalle. *Z. Anorg. Allg. Chem.*, **333** (1964) 188–200.
23. PIZZINI, S., MORLOTTI, R. & WAGNER, V., Study of the lithium oxide–nickel oxide system. *J. Electrochem. Soc.*, **116** (1969) 915–920.
24. PIZZINI, S., MORLOTTI, R. & WAGNER, V., *Phase Diagrams for Ceramists*, Vol. IV. The American Ceramic Society, Columbus, OH, 1981, Fig. 5071.
25. ANTOLINI, E., Formation of $Li_xNi_{1-x}O$ solid solution from Ni/$Li_2CO_3$ mixtures. *Mater. Lett.*, **16** (1993) 286–290.

26. MARINI, A., BERBENNI, V., MASSAROTTI, V., FLOR, G., RICCARDI, R. & LEONINI, M., Solid-state reaction study on the system Ni–$Li_2CO_3$. *Solid State Ionics*, **32–33** (1989) 398–408.
27. SATA, T., Vaporization rates from sintered bodies and single crystals of NaCl in flowing air. *J. Mater. Sci.*, **27** (1992) 2946–2951.
28. KUIPER, P., KRUIZINGER, G., GHIJSEN, J., SAWATZKY, G. A. & VERWEIJ, H., Character of holes in $Li_xNi_{1-x}O$ and their magnetic behaviour. *Phys. Rev. Lett.*, **62** (1989) 221–224.
29. LAMOREAUX, R. H. & HILDENBRAND, D. L., High temperature vaporization behaviour of oxides—I. Alkali metal binary oxide. *J. Phys. and Chem. Ref. Data*, **13** (1984) 151–172.
30. CHASE, M. W., Jr, DAVIES, C. A., DOWNEY, J. R., Jr, FRURIP, D. C., McDONALD, R. A. & SYVERUD, A. N., JANAF thermochemical table. *J. Phys. and Chem. Ref. Data*, 14 (Suppl. 1) (1985) 1429, 1441, 1444, 1446.
31. UEMATSU, K., COBLE, R. L. & BOWEN, H. K., Grain boundary segregation of $Li_2O$ in NiO. *Adv. in Ceramics*, **6** (1983) 274–288.